Divalent Rare Earth Spectra Selection Rules and Spectroscopy of $SrCl_2:Sm^{2+}$†

J. D. Axe and P. P. Sorokin
Thomas J. Watson Research Center, International Business Machines Corporation, Yorktown Heights, New York

(Received 26 October 1962)

Selection rules for vibronic transitions appearing in $4f \rightarrow 4f$ fluorescence of divalent rare earth (RE^{2+}) ions in alkaline-earth halide lattices are derived. These are applied to the cases of $SrF_2:Sm^{2+}$, $SrCl_2:Sm^{2+}$, and $CaF_2:Tm^{2+}$. On the basis of a simple theory which is outlined, selection rules for nonradiative (relaxation) transitions of RE^{2+} ions in $m3m$ symmetry are also presented. From these rules one can predict instances where spectral broadening of fluorescent lines should occur due to spontaneous emission of phonons, with consequent lifetime broadening. Comparison with experiment seems to verify these predictions. The structure of the $4f^{n-1}\,5d$ bands of RE^{2+} ions is shown to be due to vibronic coupling of pure electronic states with states involving multiquantum excitation of even-parity vibrations. Simple coupling schemes for the $4f^{n-1}\,5d$ levels are examined. Results of measurements of $SrCl_2:Sm^{2+}$ absorption and fluorescence spectra are presented. Lifetimes and quantum efficiencies are discussed.

INTRODUCTION

In connection with the development of optical masers there has recently been devoted a considerable amount of attention to the spectra of divalent rare earths (RE^{2+}) in alkaline earth halide lattices.[1–11] A few good early spectroscopic studies of these systems existed[12–14] but, by and large, spectroscopy of rare earth ions in the last two or three decades has been primarily concerned with the trivalent state (RE^{3+}). Partially this has been a result of the fact that it was generally believed that the only rare earths which could be made divalent were Eu^{2+}, Sm^{2+}, Yb^{2+}, and Tm^{2+}. The recent work of the RCA group[5–7] has now shown that other rare earths, including Dy^{2+} and Er^{2+}, can be stabilized in the divalent state in alkaline earth halide lattices.

From a theoretical standpoint these systems are of interest because of the high symmetry ($m3m$ or, in the earlier Schönflies notation, O_h) characterizing the crystalline field acting on the divalent ion. The various selection rules for transitions between energy levels of RE^{2+} ions assume the simplest of forms in this symmetry. This has already been noted[4,7] for the static-lattice $4f^n$ radiative transitions which are necessarily magnetic dipole (m.d.) in character, since RE^{2+} ions have inversion symmetry in these systems.

In this paper it is observed that the "extra lines" appearing in fluorescence as long-wavelength satellites of parent m.d. transitions obey relatively straightforward selection rules. These satellite lines have been interpreted in a general way[4,7] to be forced-electric-dipole transitions resulting from the presence of lattice vibrations, but no specific calculations were performed. Here calculations are first made for $SrF_2:Sm^{2+}$, where the close proximity of the low-lying ($4f^5 5d$) bands to the fluorescent ($4f^6, {}^5D_0$) A_{1g} state particularly simplifies the situation. Comparison with experiment leads to tentative assignments of observed vibronic components with normal modes of the XY_8 complex formed by a Sm^{2+} ion and the eight surrounding fluorines. These assignments are then checked against the fluorescent data of $CaF_2:Tm^{2+}$ and agreement seems to result.

Another general selection rule which can be tested in these systems determines whether or not symmetry allows a nonradiative (relaxation) transition to occur between two levels whose eigenfunctions transform according to definite irreducible representations of the crystal-field point group. The same vibronic interaction Hamiltonian which must be considered in the theory of the forced-electric-dipole spectrum also applies here, but in contrast to the former situation, here the even-parity terms are most important, at least when the two levels in question belong to the same configuration. Two cases are cited as examples. One is the nonradiative (n.r.) transition $({}^2F_{7/2})G \rightarrow ({}^2F_{7/2})E_{5/2}$ occurring in $CaF_2:Tm^{2+}$ which is shown to be symmetry allowed; the other is the n.r. transition in $SrF_2:Sm^{2+}$, $CaF_2:Sm^{2+}$ $({}^7F_1)T_{1g} \rightarrow ({}^7F_0)A_{1g}$ which turns out to be symmetry disallowed, at

† This research was supported jointly by International Business Machines Corporation and the United States Army Research Office, Durham, North Carolina.

[1] P. P. Sorokin and M. J. Stevenson, IBM J. Res. Develop. **5**, 56 (1961).
[2] W. Kaiser, C. G. B. Garrett, and D. L. Wood, Phys. Rev. **123**, 766 (1961).
[3] P. P. Sorokin, M. J. Stevenson, J. R. Lankard, and G. D. Pettit, Phys. Rev. **127**, 503 (1962).
[4] D. L. Wood and W. Kaiser, Phys. Rev. **126**, 2079 (1962).
[5] Z. J. Kiss and R. C. Duncan, Jr., Proc. I. R. E. **50**, 1531 (1962).
[6] Z. J. Kiss and R. C. Duncan, Jr., Proc. I. R. E. **50**, 1532 (1962).
[7] Z. J. Kiss, Phys. Rev. **127**, 718 (1962).
[8] P. P. Feofilov and A. A. Kaplyanski, Opt. Spectr. **12**, 272 (1962).
[9] G. H. Dieke and R. Sarup, J. Chem. Phys. **36**, 371 (1962).
[10] J. R. O'Connor and H. A. Bostick, J. Appl. Phys. **33**, 1868 (1962).
[11] W. A. Runciman and C. V. Stager, J. Chem. Phys. **37**, 196 (1962).
[12] S. Freed and S. Katcoff, Physica **14**, 17 (1948).
[13] F. D. S. Butement, Trans. Faraday Soc. **44**, 617 (1948).
[14] P. P. Feofilov, Opt. i Spektroskopiya **1**, 992 (1956).

least in the order of approximation of the theory proposed here. Significantly, the $(^2F_{7/2})G$ level shows clear evidence of lifetime broadening due to spontaneous emission of phonons, whereas the $(^7F_1)T_{1g}$ level does not. Since $(^7F_1)T_{1g}$ and $(^7F_0)A_{1g}$ are, respectively, terminal and ground states of Sm^{+2} four-level masers, forbiddenness of n.r. transitions between these states may explain a cutoff phenomenon observed in $CaF_2:Sm^{2+}$ masers[1,2] plausibly associated with "jamming" of the terminal state.

Some considerations are made about the width of the $4f \rightarrow 5d$ pumping bands in these systems. The absorption spectrum of $SrCl_2:Sm^{2+}$ gives clear evidence that the ≈ 500 cm^{-1} wide Sm^{2+} "bands" consist of a series of vibronic satellites of allowed parent electric-dipole (e.d.) transitions $(^7F_0)A_{1g} \rightarrow (4f^5\,5d)T_{1u}$. In contrast to the case of vibronic transitions appearing in fluorescence and associated with transitions lying wholly within the $4f$ shell, these vibronic transitions are characterized by large changes in vibrational quantum numbers and by the parent and satellite lines having more-or-less equal intensities. The mechanism which operates here is apparently the one originally suggested by Van Vleck.[15]

In connection with the discussion of the $5d$ bands it is pointed out that the coupling scheme suggested by the authors of reference 4 can be amended to fit certain known experimental facts.[11]

Finally, a spectroscopic study of the fluorescence of the system $SrCl_2:Sm^{2+}$ is described. The results are quite similar to those found in the case of $SrF_2:Sm^{2+}$.

VIBRONIC TRANSITIONS IN $4f \rightarrow 4f$ SPECTRA

A good example of forced-electric-dipole transitions occurs in the luminescence spectrum of Sm^{2+} in SrF_2. At low temperatures (4.2°K) the fluorescence appears as a series of sharp magnetic dipole transitions $^5D_0 \rightarrow {}^7F_i$ with the $^5D_0 \rightarrow {}^7F_1$ line being a hundred times or so more intense than the other ones. However, at 4.2°K there is, in addition, a group of lines on the long-wavelength side of each sharp line, about as intense as the weaker $^5D_0 \rightarrow {}^7F_i$ transitions, but not as sharp. These "extra lines" are forced-electric-dipole transitions. For $SrF_2:Sm^{2+}$ a progression of satellites with an average spacing of 90, 140, 216, 282, and 349 cm^{-1} from each sharp m.d. line is observed. The relative intensities of all these lines are given in Table III of reference 4. Here we attempt to account for the observed values.

The relevant formal theory can be expressed rather easily.[15–18] Here Satten's treatment is followed. The vibrational-electronic interaction $\mathcal{H}'$ may be written

$$\mathcal{H}' = -\sum_k Q_k v_k', \tag{1}$$

where the sum is over the normal vibrational coordinates Q_k of the XY_8 complex and v_k' is a function of the coordinates of the $4f$ electrons of the central ion. The latter function transforms under central ion $4f$ electron coordinate transformations according to the same representation as Q_k.[18] This fact enables one to find the vibronic selection rules without knowing in detail the characteristic displacements of the normal modes. It is only necessary to determine the irreducible representations to which the modes belong.

Group theory shows that for the XY_8 complex, the normal modes are given by

$$D_{\text{vib}} = A_{1g}+A_{2u}+E_g+E_u+2T_{1u}+2T_{2g}+T_{2u}. \tag{2}$$

There are thus five ungerade vibrations, which fact conveniently accounts for the number of observed vibronic components in the fluorescence spectrum of $SrF_2:Sm^{2+}$.

Consider the matrix elements of components of the electric dipole moment operator between the ground state and some excited state. For a modified excited state involving one quantum of excitation of the mode with normal coordinate Q_r coupled to the purely electronic state u_e one writes

$$\psi_e = u_e\eta_1(Q_r) - \sum_n \frac{\langle u_n\eta_0(Q_r)|\mathcal{H}'|u_e\eta_1(Q_r)\rangle}{E_n-E_e} u_n\eta_0(Q_r) - \sum_n \frac{\langle u_n\eta_2(Q_r)|\mathcal{H}'|u_e\eta_1(Q_r)\rangle}{E_n-E_e} u_n\eta_2(Q_r). \tag{3}$$

Likewise, the modified ground state is, assuming no quanta of vibration to be present in the state,

$$\psi_g = u_g\eta_0(Q_r) - \sum_n \frac{\langle u_n\eta_1(Q_r)|\mathcal{H}|u_g\eta_0(Q_r)\rangle}{E_n-E_g} u_n\eta_1(Q_r). \tag{4}$$

Let P_ϵ = be a typical component of the electric dipole moment operator $P=\sum_j e\mathbf{r}_j$. Its matrix element is found to be, using Eqs. (3) and (4), and choosing only $k=r$ in Eq. (1)

$$\langle\psi_e|P_\epsilon|\psi_g\rangle = \sum_n \frac{\langle u_n|v_r'|u_g\rangle\langle u_e|P_\epsilon|u_n\rangle}{E_n-E_g}\left(\frac{\hbar}{2\nu_r}\right)^{1/2} + \sum_n \frac{\langle u_n|v_r'|u_e\rangle\langle u_n|P_\epsilon|u_g\rangle}{E_n-E_e}\left(\frac{\hbar}{2\nu_r}\right)^{1/2}. \tag{5}$$

In Eq. (5) the matrix elements of Q_r have been evaluated. They are

$$\langle\eta_{n-1}(Q_r)|Q_r|\eta_n(Q_r)\rangle = \langle\eta_n(Q_r)|Q_r|\eta_{n-1}(Q_r)\rangle = \left(\frac{n\hbar}{2\nu_r}\right)^{1/2}. \tag{6}$$

The energy of the nuclear system is given by

$$\mathcal{H}_{\text{nucl}} = \sum_k \tfrac{1}{2}\dot{Q}_k^2 + \nu_k^2 Q_k^2. \tag{7}$$

In the expression (1) for the interaction Hamiltonian it is assumed that the crystal field acting on the RE^{2+} ion arises entirely from the nearest neighbor anions.

[15] J. H. Van Vleck, J. Phys. Chem. **41**, 67 (1937).
[16] R. A. Satten, J. Chem. Phys. **27**, 286 (1957).
[17] R. A. Satten, J. Chem. Phys. **29**, 658 (1958).
[18] R. A. Satten, J. Chem. Phys. **30**, 590 (1959).

Parity remains a rigorous quantum number for the wave functions of the various configurations of RE^{2+} ions in alkaline earth fluoride lattices, again by virtue of the inversion symmetry present. In applications of Eq. (5) to RE^{2+} spectra the predominantly contributing wave functions u_n are the $4f^{n-1}\,5d$ orbitals of the lowest lying pumping bands and u_e, u_g are $4f^n$ orbitals. The functions u_n are of odd parity and u_g, u_e are even except in the rather unique case of $CaF_2:Sm^{2+}$. With the above specifications for the wave functions it follows that $\langle u_e|P_\epsilon|u_n\rangle$, $\langle u_n|P_\epsilon|u_g\rangle$ can be both nonzero. Therefore, for $\langle\psi_e|P_\epsilon|\psi_g\rangle$ to be nonzero, v_r' must have odd parity also. Hence, ungerade vibrations in Eq. (2) are the ones of importance.

The vibronic selection rules for RE^{2+} transitions lying wholly within the $4f$ shell may now be examined. In $m3m$ symmetry, P_ϵ transforms as T_{1u}. If one considers, first of all, the system $SrF_2:Sm^{2+}$, the main contribution to Eq. (5) comes from the second term, because of the relative smallness of E_n-E_e compared to E_n-E_g. The excited state u_e is $(4f^6, {}^5D_0)A_{1g}$ and is located 14 616 cm^{-1} above the true Sm^{2+} ground state $(4f^6, {}^7F_0)A_{1g}$. For the state u_g appearing in Eq. (5) the various ^7F terms can be tried, including the maser terminal state $(4f^6, {}^7F_1)T_{1g}$ located only 263 cm^{-1} above the ground state. The "edge" of the red $5d$ band appears at 15 066 cm^{-1} and is thus only 450 cm^{-1} above u_e while being 14 803 cm^{-1} above u_g, when the latter is taken to be $(^7F_1)T_{1g}$.

The wave functions u_n are assumed to transform according to representations which include all possible ungerade $m3m$ irreducible representations. A plausible coupling scheme suggested below predicts, in fact, that the lowest lying $4f^5\,5d$ states transform as

$$A_{1u}+A_{2u}+2E_u+3T_{1u}+3T_{2u}.$$

The nonzero matrix elements occurring in Eq. (5) can, with the aid of a multiplication table for irreducible representations, be easily spotted. The results are summarized in Table I for $SrF_2:Sm^{2+}$. Here u_e transforms, of course, as A_{1g}.

Comparison of Table I with experimental data should allow assignments of vibronic lines to be made. One is tempted to associate the five vibronic transitions at 14 530 cm^{-1} (12), 14 470 cm^{-1} (2), 14 390 cm^{-1} (140), 14 325 cm^{-1} (375), and 14 260 cm^{-1} (20), with the sharp (forbidden) parent magnetic dipole line $(^5D_0)A_{1g}\rightarrow(^7F_0)A_{1g}$ appearing at 14 616 cm^{-1}. (The data are taken from Table III of reference 4; the numbers in parentheses are relative intensities.) The spacings from the parent line are 86, 146, 226, 291, and 356 cm^{-1}, in agreement with the average spacings. Then from Table I, the third and fourth lines would appear to be due to the (two) T_{1u} vibrational modes. The fifth vibronic line associated with the parent lines at 14 616 cm^{-1} $[u_g=(^7F_0)A_{1g}]$, 14 353 cm^{-1} $[u_g=(^7F_1)T_{1g}]$, and 13 581 cm^{-1} $[u_g=(^7F_2)E_g]$ is in each case small, in contrast to the situation involving the parent line at 13 964 cm^{-1} $[u_g=(^7F_2)T_{2g}]$. The fifth line, then, probably corresponds to the A_{2u} mode. The first satellite of the 13 581 cm^{-1} m.d. line is small and, therefore, probably corresponds to E_u. This would, by the process of elimination, identify the second vibronic line in each group as T_{2u}. These assignments should be regarded as somewhat tentative, although they seem to be consistent with the situation in $CaF_2:Tm^{2+}$, as we now show.

In $CaF_2:Tm^{2+}$ the low-temperature fluorescence $^2F_{5/2}\rightarrow{}^2F_{7/2}$ is concentrated in two sharp static-lattice m.d. transitions: $(^2F_{5/2})E_{5/2}\rightarrow(^2F_{7/2})G$ and $(^2F_{5/2})E_{5/2}\rightarrow(^2F_{7/2})E_{5/2}$. In the vibronic structure accompanying each of these parent lines there is present a prominent line displaced from the parent one by about 90 cm^{-1}. This should be the E_u vibration. A prominent line occurs about 350 cm^{-1} away from $(^2F_{5/2})E_{5/2}\rightarrow(^2F_{7/2})G$ but is not observed at this distance from $(^2F_{5/2})E_{5/2}\rightarrow(^2F_{7/2})E_{5/2}$. This should be associated with the vibration A_{2u}.

Considering Eq. (5) and making the specifications $u_e(^2F_{5/2})E_{5/2}$; $u_g=(^2F_{7/2})E_{5/2}$, $(^2F_{7/2})G$; $u_n=E_{5/2u}$, G_u leads to the prediction that the E_u vibronic component should be seen in both cases while the A_{2u} vibronic line should accompany only the first transition. Hence, it appears that the vibrational assignments made on the basis of the Sm^{2+} data explain also the Tm^{2+} data.

TABLE I. Symmetry-allowed and symmetry-forbidden vibronic transitions in fluorescence of $SrF_2:Sm^{2+}$. Only the second term in Eq. (5) is considered.

Representation of Q_r	Representation of u_g			
	T_{1g}	T_{2g}	E_g	A_{1g}
A_{2u}	f	a	f	f
E_u	a	a	f	f
T_{1u}	a	a	a	a
T_{2u}	a	a	a	f

NONRADIATIVE TRANSITIONS

The orbit-lattice interaction which induces nonradiative (relaxation) transitions between Stark components of $4f^n$ levels or between close-lying $4f^n$ levels of different multiplets is again the same Hamiltonian expressed in Eq. (1), provided it is assumed that fluctuations in the part of the crystal field due to the nearest neighbors are primarily responsible for the nonradiative transitons. However, at least for nonradiative transitions between states of the same configuration, the terms in Eq. (1) which are effective are now the even parity ones. These are often referred to as the Jahn-Teller distortions.

Consider two levels, e and g, belonging to the same $4f^n$ configuration and suppose that the energy separation Δ is smaller than the cutoff of the Debye spectrum of the crystal so that single acoustical phonons with energy $\doteq\Delta$ can induce transitions. For the case of a simple cubic lattice, for which there are six octahedrally

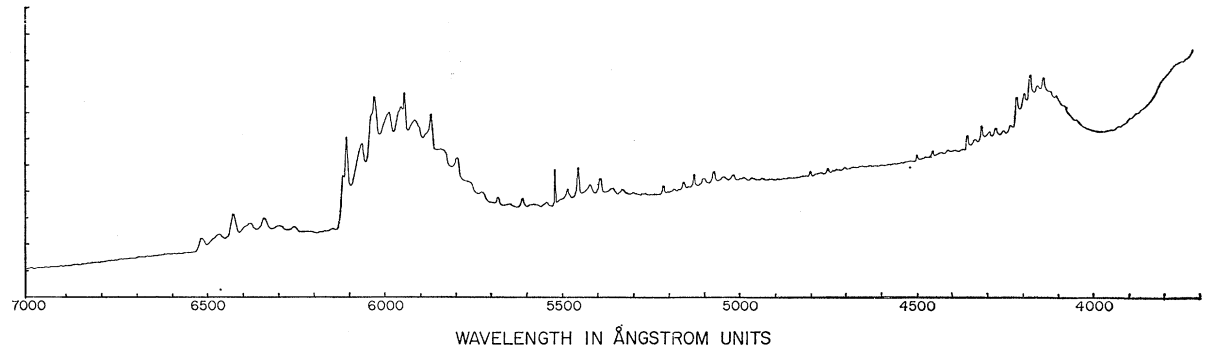

FIG. 1. Absorption spectrum at 4.2°K of $SrCl_2:Sm^{2+}$ showing general structure.

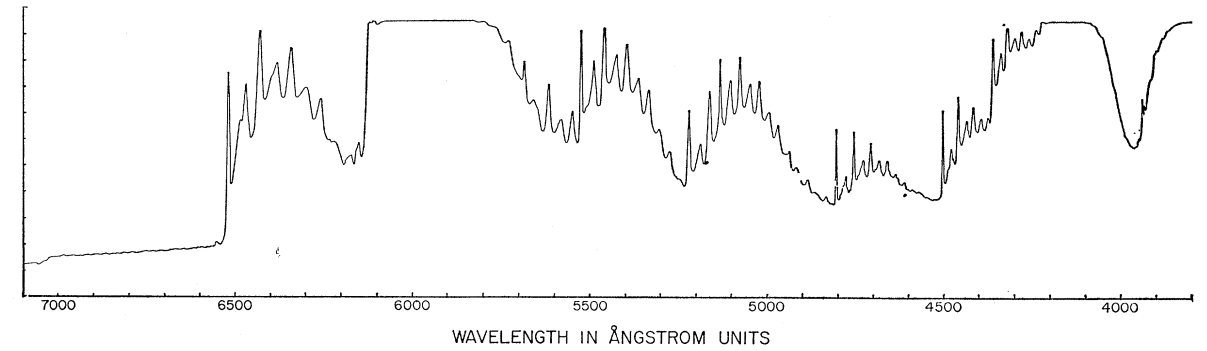

FIG. 2. Absorption spectrum at 4.2°K of $SrCl_2:Sm^{2+}$ showing detailed structure.

coordinated nearest neighbors (XY_6), one can make use of Van Vleck's calculations[19] to derive the expressions

$$W_{g\to e}=\frac{256\pi^7R^2\Delta^3}{3v^5\rho h^4}\left(\frac{1}{e^{\Delta/kT}-1}\right)\sum_k|\langle\psi_e|v_k'|\psi_g\rangle|^2, \quad (8)$$

and

$$W_{e\to g}=\frac{256\pi^7R^2\Delta^3}{3v^5\rho h^4}\left(\frac{e^{\Delta/kT}}{e^{\Delta/kT}-1}\right)\sum_k|\langle\psi_e|v_k'|\psi_g\rangle|^2, \quad (9)$$

for the upward and downward transition probabilities, respectively. The expressions (8) and (9) are the rates which enter in Orbach's two-step process used to explain paramagnetic relaxation of the Zeeman-split components of ground states.[20] As $T\to 0$, $W_{g\to e}$ becomes vanishingly small, whereas $W_{e\to g}$ tends to a constant value, proportional to the cube of the energy separation Δ. In Eqs. (8) and (9) it is assumed that $v_l=v_t=v$, where v_l and v_t are, respectively, the velocities for longitudinal and transverse waves. In these equations ρ is the crystal density, $2R$ is the cross-sectional dimension of the complex. Formulas (8) and (9) are assumed to contain the essential features to explain the XY_8 case also.

The limit: $W_{e\to g}$ as $T\to 0$ corresponds to spontaneous emission of phonons and if it is large enough, lifetime broadening of the level e can result.[21]

For Sm^{2+} in alkaline earth halide lattices the n.r. transition $(^7F_1)T_{1g}\to(^7F_0)A_{1g}$ is, in the order of the approximation of this theory, forbidden because $\sum_k|\langle\psi_e|v_k'|\psi_g\rangle|^2=0$. This can be easily seen since the product of the representations of ψ_e, ψ_g transforms according to

$$T_{1g}\times A_{1g}=T_{1g},$$

and, as Eq. (2) shows, T_{1g} is not one of the XY_8 vibrations. Thus, nonradiative transitions from terminal to ground states of $CaF_2:Sm^{2+}$, $SrF_2:Sm^{2+}$ optical masers are forbidden in first order, although the energy separation Δ is 263 cm^{-1}, which is well below the Debye cutoff, estimated to be 420 cm^{-1}.

A characteristic feature noted[1,2] in pulsed operation of $CaF_2:Sm^{2+}$ masers is that oscillation ceases at higher pump light levels than present at the start of the maser burst. It is likely, in view of the preceding calculation, that this phenomenon is due to filling the $^7F_1$ level.

It is also observed that the width of the $(^5D_0)A_{1g}\to(^7F_1)T_{1g}$ transition is only $\doteq 0.5$ cm^{-1} in $SrF_2:Sm^{2+}$ and $SrCl_2:Sm^{2+}$. There is, thus, no evidence of pronounced lifetime broadening such as exists in the case of the 8410 cm^{-1} $(^2F_{5/2})E_{5/2}\to(^2F_{7/2})G$ transition in $CaF_2:Tm^{2+}$. This static-lattice m.d. transition has a 4.2°K linewidth of 12 cm^{-1} while the other symmetry-allowed m.d. transition, $(^2F_{5/2})E_{5/2}\to(^2F_{7/2})E_{5/2}$, has a width of only 0.3 cm^{-1} at the same temperature. In agreement with this line of argument, calculation shows that the n.r.

[19] J. H. Van Vleck, Phys. Rev. **57**, 426 (1940).
[20] C. B. P. Finn, R. Orbach, and W. P. Wolf, Proc. Phys. Soc. (London) **77**, 2617 (1961).
[21] S. Yatsiv, Physica **28**, 521 (1962).

transition $(^2F_{7/2})G \rightarrow (^2F_{7/2})E_{5/2}$ is allowed, being induced by spectral components at Δ of the $(XY_8)E_g$ and T_{2g} normal mode displacements. This spontaneous emission of phonons broadens the 8410 cm^{-1} line.

VIBRONICALLY COUPLED $4f^{n-1}\,5d$ STATES

Figures 1 and 2 show the absorption spectra at 4.2°K of $SrCl_2:Sm^{2+}$. Pictures of the absorption spectrum of $SrF_2:Sm^{2+}$ are found in references 3 and 4.

The $SrCl_2$ traces show an unusually pronounced vibrational structure. Each "band," for example, the one spanning the region 6200–6550 Å, is evidently composed of a number of sets of vibronic transitions having successive components spaced approximately 213 cm^{-1} apart. The first line of each set is the sharpest, the lines becoming successively broader for higher energy components of a set. In Sm^{2+} the first line of each set corresponds to a transition from the ground state to a $(5d)T_{1u}$ level. From Figs. 1 and 2 it would appear that the typically observed widths of several hundreds of cm^{-1} for the $5d$ pumping bands of RE^{2+} ions in alkaline earth halide lattices result from the series of vibronic lines $n=1, 2, 3, 4, \cdots$ accompanying each of the parent e.d. lines, $(^7F_0)A_{1g} \rightarrow (5d)T_{1u}$ in the case of Sm^{2+}. In $SrCl_2:RE^{2+}$ these vibronic lines are well resolved. However, in both $SrF_2:Sm^{2+}$ and $CaF_2:Sm^{2+}$ there is also observed a constantly recurring frequency ν_r. In these systems its values are 292 and 335 cm^{-1}, respectively.[3]

The theory most applicable here was first roughly sketched by Van Vleck.[15] Consider an electronic plus vibrational level B which lies near a pure electronic level A. Van Vleck indicated that the vibrational-electronic interaction, here much greater than for $4f^n$ states (since a $5d$ electron is involved), can couple the states A and B causing them to lose their separate identity, each one taking on some character of the other.

Suppose, for definiteness, A is a $(5d)T_{1u}$ state of Sm^{2+}: $\phi_A=u_A\eta_0(Q_r)$, and B is the state: $\phi_B=u_A\eta_1(Q_r)$, and C is the state: $\phi_C=u_A\eta_2(Q_r)$, and so on. The perturbed states are then approximately of the form

$$\phi_A' \doteq \phi_A - \frac{\langle u_A\eta_1(Q_r)|\mathcal{H}'|u_A\eta_0(Q_r)\rangle}{h\nu_r}\phi_B,$$

$$\phi_B' \doteq \phi_B + \frac{\langle u_A\eta_0(Q_r)|\mathcal{H}'|u_A\eta_1(Q_r)\rangle}{h\nu_r}\phi_A + \frac{\langle u_A\eta_2(Q_r)|\mathcal{H}'|u_A\eta_1(Q_r)\rangle}{h\nu_r}\phi_C. \quad (10)$$

Electric dipole transitions from the ground state to the state $\phi_{B'}$ are now possible because of the admixture of ϕ_A. If the interaction energy becomes a sizeable fraction of the vibrational splitting $h\nu_r$, the perturbation approximation [Eq. (10)] breaks down, and all vibronic levels of u_A are coupled together, accounting for the observed vibrational structure. It will be recognized that this is the same mechanism that gives rise to the characteristic band structure of polyatomic molecules.

The vibronic Hamiltonian $\mathcal{H}'$, although different in the case of $4f^{n-1}\,5d$ states from that for $4f^n$ levels, is still given basically by Eq. (1), again linear in the Q_r. Here the even parity terms are of interest. These are A_{1g}, E_g, T_{2g}. For Sm^{2+}, an argument used in reference 11 shows that the $2T_{2g}$ vibrations contribute negligibly to the vibronic interaction and can probably be neglected. Thus, the 213 cm^{-1} frequency must be the resonant frequency of either the A_{1g} or E_g normal modes. It is not immediately apparent why one or the other of these modes should predominantly make its influence felt in the absorption spectrum. The A_{1g} vibration involves a simple change in dimension of the XY_8 cube and couples the vibronic levels of T_{1u} together without removing the T_{1u} degeneracy. The E_g vibrations couple the vibronic levels of T_{1u} together by causing the T_{1u} states to split. The theoretical problem involved here is close to that which occurs in the so-called "dynamic Jahn-Teller effect."[22]

Since the same interval $\doteq 213$ cm^{-1} occurs in absorption in $SrCl_2:Eu^{2+}$, it is of interest to examine whether A_{1g} and E_g vibrations could be effective in this case. The ground state of Eu^{2+} is $(^8S_{7/2})E_{1/2g}+E_{5/2g}+G_g$. These components are all close lying to each other and are all occupied, even at 4.2°K. Electric dipole transitions are allowed from these states to $4f^{n-1}\,5d$ states transforming as $E_{1/2u}$, $E_{5/2u}$, or G_u. All three excited states could be coupled to their vibrational satellite levels by A_{1g}, but only G would be coupled to its vibrational satellite levels by E_g. Since not all absorption bands of $SrCl_2:Eu^{2+}$ show the 213 cm^{-1} interval,[12] it would seem that the E_g vibration is responsible for the vibronic structure.

Further evidence that E_g rather than A_{1g} is the vibrational mode responsible for the coupling is the fact that at 4.2°K the fluorescence $(5d)A_{1u} \rightarrow (^7F_1)T_{1g}$ in $CaF_2:Sm^{2+}$ primarily occurs in a single sharp line, without the accompaniment of an intense long-wavelength continuum, persisting down to the lowest temperatures, such as occurs in the fluorescence spectrum of Eu^{2+}. Since $A_{1u}\times A_{1u}=A_{1g}$, the situation as exists in $CaF_2:Sm^{2+}$ would be expected if A_{1g} modes were not active in vibronic coupling. For Eu^{2+}, on the other hand, the emitting state, believed to be a $(4f^6\,5d)G$ state, could be vibronically coupled to its higher energy vibrational satellites by E_g modes. The lowest lying $(4f^6\,5d)G$ wave function would then be a linear combination of the configurational wave functions: $\eta_0(Q_r)$, $\eta_1(Q_r)$, $\eta_2(Q_r), \cdots$ etc., and allowed e.d. transitions from this state could occur to the various (uncoupled) vibrational states of the ground state $[u_g=(4f^7, {}^8S_{7/2})E_{5/2}+E_{1/2}+G]$: $u_g\eta_0(Q_r)$, $u_g\eta_1(Q_r)$, $u_g\eta_2(Q_r), \cdots$, etc. That the 4.2°K fluorescence continuum of $CaF_2:Eu^{2+}$ is, indeed, comprised of such transitions as described here becomes evident upon examination of the 4.2°K fluorescence spectrum of

[22] H. C. Longuet-Higgins, U. Öpik, M. H. L. Pryce, and R. A. Sack, Proc. Roy. Soc. (London) A244, 1 (1958).

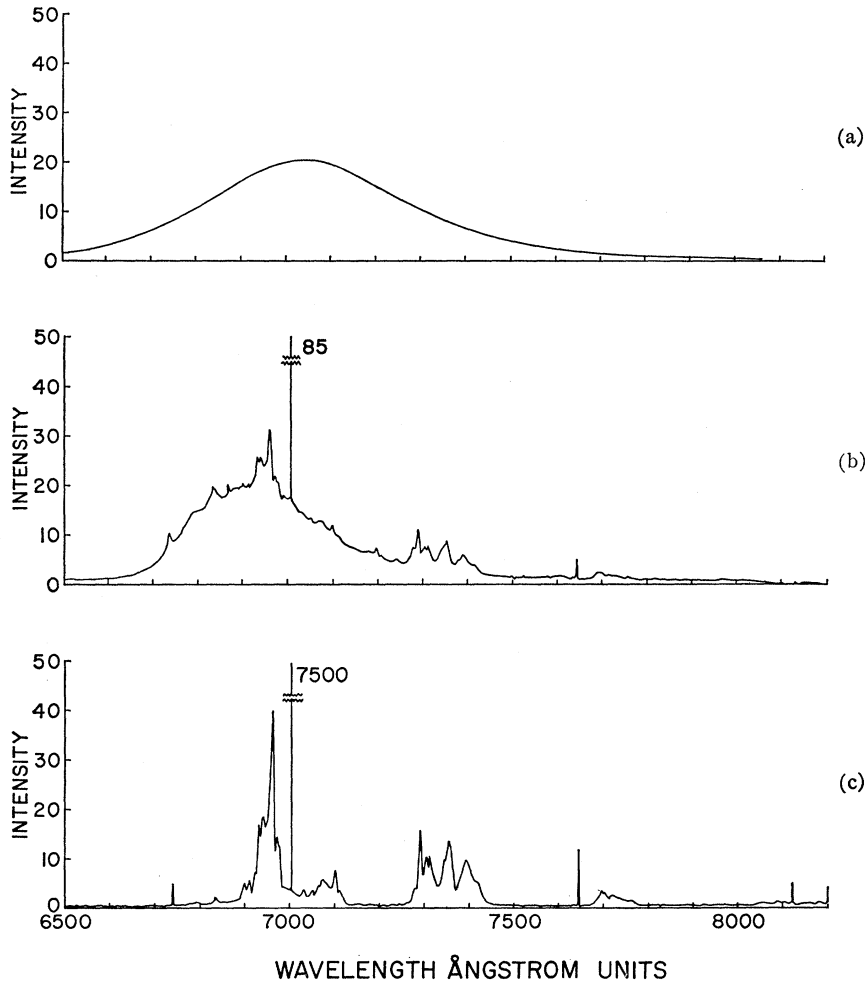

FIG. 3. Fluorescence of $SrCl_2:Sm^{2+}$; (a) 300°K, (b) 77°K, (c) 4.2°K.

$SrCl_2:Eu^{2+}$, where the vibronic components (213 cm^{-1} spacing) are clearly resolved. The relative sharpness of $4f^{n-1}\,5d \rightarrow 4f^n$ vibronic components in RE^{2+} spectra in different lattices having $m3m$ symmetry is a measure of the damping of XY_8 modes due to lattice coupling.

This line of argument appears to explain the high-temperature broad-band fluorescence in Sm^{2+} (Fig. 3), for this emission very likely originates from the lowest $(4f^6\,5d)T_{1u}$ state which is coupled to its vibronic satellites by $(XY_8)E_g$ modes and, hence, would be expected to give rise to a series of vibronic fluorescent transitions, in the manner of Eu^{2+}. In the lattices CaF_2, SrF_2, and $SrCl_2$, the T_{1u} state becomes thermally occupied only at temperatures well above 4.2°K hence the continuum vanishes at this temperature.

COUPLING SCHEMES FOR $4f^{n-1}\,5d$ CONFIGURATIONS

When an electron in $SrF_2:Sm^{2+}$ is promoted from the $4f$ shell it leaves behind five electrons in what (presumably) is the lowest $4f^5$ term. This is known to be $^6H_{5/2}$ (from Sm^{3+}). The wave function for the promoted ($5d$) electron transforms as $E_g \times D^{(1/2)} = G$. Now the question is: How are the electrons of the $4f^5$ configuration coupled with the promoted electron?

Two simple schemes suggest themselves: (a) the interaction of the $4f^5$ electron shell with the $m3m$ crystal field may be considered stronger than the interaction of this same shell with the promoted $5d$ electron or (b) the reverse.

Consider scheme (a). In cubal coordination $^6H_{5/2}$ splits into an $E_{5/2}$ state and a G state, with $E_{5/2}$ lowest. Thus, taking the lowest state of this configuration and coupling it to the $5d$ electron state G, the combined wave function transforms as

$$G \times E_{5/2} = E_u + T_{1u} + T_{2u},$$

which is the scheme proposed in reference 4 for the lowest lying states of the $5d$ band.

Alternatively, in scheme (b) one neglects the effect of the $m3m$ crystal field on the $^6H_{5/2}$ state and couples the latter instead to the $5d$ electron. This leads to the representation for the combined wave function

$$G \times D^{(5/2)} = A_{1u} + A_{2u} + 2E_u + 3T_{1u} + 3T_{2u}.$$

TABLE II. The fluorescence spectrum of $SrCl_2:Sm^{2+}$ at 4°K.

Air (Å)	Vac (cm^{-1})	I	Air (Å)	Vac (cm^{-1})	I
8119	12 319	4(*s*)	7064	14 160	5
7765	12 881	1	7050	14 188	3
7725	12 948	2	7031	14 226	4
7719	12 958	2	7006	14 277	7×10^3(*s*)
7702	12 987	3	6975	14 341	12
7694	13 000	4	6969	14 353	15
7643	13 087	12(*s*)	6958	14 376	40
7414	13 491	4	6939	14 415	18
7391	13 533	9	6929	14 436	17
7352	13 607	12	6923	14 448	7
7347	13 614	9	6910	14 475	5
7341	13 625	8	6898	14 501	4
7309	13 685	10	6833	14 639	1
7303	13 696	10	6792	14 727	0.5
7289	13 726	15	6739	14 843	4(*s*)
7277	13 745	5			
7241	13 814	0.5(*s*)			
7109	14 070	3			
7099	14 090	7			
7075	14 138	5			

Since there is direct evidence[11] from strain measurements in $CaF_2:Sm^{2+}$ that the lowest lying state of the 5*d* band is an A_{1u} state, this would indicate a strong preference for scheme (b). Scheme (b) is also more reasonable on *a priori* grounds.[23]

FLUORESCENCE OF $SrCl_2:Sm^{2+}$

Since good single crystals of $SrCl_2$ are relatively easy to grow and since divalent samarium is rather easily incorporated into this crystal, forming a luminescent solid which is visually very bright even at room temperature (in contrast to $CaF_2:Sm^{2+}$, $SrF_2:Sm^{2+}$ which do not fluoresce at all at 300°K), a brief study was made of the fluorescence of $SrCl_2:Sm^{2+}$. We find, on the whole, an expected rather close similarity to the spectral characteristics of $SrF_2:Sm^{2+}$. The latter have been already studied in great detail[3,4,8] and hence the $SrCl_2:Sm^{2+}$ spectra will be only briefly discussed.

In Figs. 3(a)–(c) the luminescence of $SrCl_2:Sm^{2+}$ is shown (on the same scale) at temperatures 300, 77, 4.2°K, respectively. Table II indicates the exact positions of the lines appearing in the 4.2°K spectrum.

The general features of the spectrum have the same interpretation as in $SrF_2:Sm^{2+}$. These are three weak sharp lines present in addition to the main emission line $(^5D_0)A_{1g}\rightarrow(^7F_1)T_{1g}$ which occurs at 7007 Å (14 272 cm^{-1}). Two of these are the symmetry-allowed transitions: $(^5D_0)A_{1g}\rightarrow(^7F_3)T_{1g}$ at 7644 Å (12 915 cm^{-1}) and $(^5D_0)A_{1g}\rightarrow(^7F_4)T_{1g}$ at 8119 Å (12 310 cm^{-1}). The positions of the two lower levels agree with the values generally found in Sm^{2+}. The third weak line at 6740 Å (14 839 cm^{-1}) is of too short a wavelength to be attributed to any transition originating from the $(^5D_0)A_{1g}$ level. The energy difference is very close to that expected for the electric dipole transition between the lowest lying 5*d* state $(4f^5\,5d)A_{1u}$ to the $(^7F_1)T_{1g}$ level which is responsible for maser action in $CaF_2:Sm^{2+}$ (it has also been seen weakly[4] in $SrF_2:Sm^{2+}$). It is probably rendered metastable with respect to direct nonradiative transitions to the $(^5D_0)A_{1g}$ (since $A_{1u}\times A_{1g}=A_{1u}$, an A_{1u} vibration which is not present in an XY_8 complex would be required).

We find in agreement with Butement,[13] that at room temperature no structure is present in the broad emission band which extends from about 6500 to 7700 Å peaking at ~7050 Å, rather than from 6550 to 6900 Å peaking at 6760 Å as he reported. The discrepancy lies undoubtedly in the nonlinear spectral sensitivity of his photographic detection.

A feature of the fluorescent spectrum 3(c) which differs slighly from what is observed in $SrF_2:Sm^{2+}$ is the apparent complete absence of any trace of symmetry-forbidden parent m.d. lines; that is, lines representing transitions which terminate on ^7F levels transforming as A_{1g}, A_{2g}, E_g, or T_{2g}.

The vibronic structure associated with the observed parent lines or with the positions at which parent lines would occur if they were symmetry-allowed is, unfortunately and unexplainably, more complicated than is observed in $SrF_2:Sm^{2+}$. The main source of trouble is extra lines, beyond the five which are predicted by simple theory. One can look, for example, at the vibronic structure accompanying the (forbidden) m.d. line $(^5D_0)A_{1g}\rightarrow(^7F_0)A_{1g}$. Because of the lower values of XY_8 vibrational frequencies occurring in $SrCl_2$, it is now all shifted to the high-energy side of the main emission line, showing that in $SrF_2:Sm^{2+}$ it was correct to associate the relatively strong vibronic components at 14 325 and 14 390 cm^{-1} with $(^5D_0)A_{1g}\rightarrow(^7F_0)A_{1g}$ and not with the 14 353 cm^{-1} main emission line in that system (see Table III of reference 4). One assignment scheme that can be applied to Fig. 4(c), is the following. Associate the line at 14 494 cm^{-1} (6900 Å) with E_u, the line at 14 465 cm^{-1} (6913 Å) with T_{2u}, the triplet at [14 445 cm^{-1}, 14 426 cm^{-1} (6934 Å), 14 411 cm^{-1} (6940 Å)] with one T_{1u}, the triplet at [14 372 cm^{-1} (6958 Å), 14 348 cm^{-1} (6970 Å), 14 335 cm^{-1}] with another T_{1u}, and the line appearing at 14 308 cm^{-1} on the shoulder of the main emission line with A_{2u}. This assignment is the closest to the scheme used to interpret $SrF_2:Sm^{2+}$, and the selection rules (Table I) are approximately seen to be obeyed. The spacings of the components from the parent line, assumed to be at 14 272 $cm^{-1}+278$ $cm^{-1}=14\,550$ cm^{-1}, are thus: 56, 85, 123, 198, and 215 cm^{-1}, where the T_{1u} "triplet" components have been averaged. The 278 cm^{-1} splitting is the value observed for samarium in BaF_2 which is a larger lattice than SrF_2 and thus more like $SrCl_2$. On this basis one can account for the vibronic structure accompanying the main emission line. The other groups of vibronic lines are difficult to analyze since components associated with different parent lines overlap.

Another difference between the behavior of Sm^{2+} in

[23] B. R. Judd, Phys. Rev. **125**, 613 (1962).

TABLE III. Selected data of $SrCl_2:Sm^{2+}$, $SrF_2:Sm^{2+}$.

	$SrCl_2$			SrF_2		
	$\Delta\nu$ (cm^{-1})	η_e	τ (sec)	$\Delta\nu$ (cm^{-1})	η_e	τ (sec)
221°			5×10^{-5}			
90°				1.1		
77°	0.9	0.03	7.5×10^{-3}	0.8	0.03	8×10^{-4}
20°				0.8	0.4	1×10^{-2}
4.2°	0.5	0.64	1.4×10^{-2}	0.7	0.4	1.4×10^{-2}

$SrCl_2$ and SrF_2 occurs in the lifetimes of the radiating levels of the two systems, although the linewidths and quantum efficiencies seem quite comparable. A comparison of the lifetimes, quantum efficiencies (η_e=number of photons emitted in line/total photons emitted), and linewidths of the predominant sharp emissions of Sm^{2+} in SrF_2 and $SrCl_2$ are given in Table III. Measurements made at 298, 77, and 4°K with identical illumination and collection conditions indicate that to within about 30% the total fluorescence output is independent of temperature over this range in $SrCl_2$.

The decrease in radiative lifetime with increasing temperature probably reflects the fact that the $(4f^6\,5d)A_{1u}$ state as well as the $(4f^6\,5d)T_{1u}$ state lying $\doteq 115$ cm^{-1} above it start to become thermally occupied eventually. Excited Sm^{2+} ions can thus radiate via e.d. transitions from these states to the ^7F states below, and the T_{1u} state (being vibronically coupled to its vibrational satellites) will emit in a fluorescence continuum, as pointed out above. For a large temperature range one would, therefore, roughly expect the measured lifetime τ to be reduced from its 4.2°K value by a factor equal to the ratio of the area represented by the sharp m.d. lines and their $(4f\rightarrow 4f)$ vibronic satellites divided by the total fluorescence area. This we (roughly) find to be the case. What appears strikingly in Fig. 3, however, and is not presently understood by us, is the fact that the ratio of the area represented by the main sharp m.d. line divided by the area of all the sharp m.d. lines plus their vibronic satellites is not constant, but decreases rapidly with increasing temperature. All these lines represent $4f\rightarrow 4f$ fluorescent transitions originating from the same state $(^5D_0)A_{1g}$.

It should be possible to estimate the lifetime $\tau_{m.d.}$ quite accurately since it is independent of the crystal field and depends (since the transition $^5D_0\rightarrow{}^7F_1$ is spin forbidden) upon the spin-orbit admixing of the septet and quintet states. These intermediate coupling calculations have been carried out by Ofelt[24] and using his eigenfunctions we calculate $\tau_{m.d.}=7.5\times10^{-2}$ sec being, of course, temperature independent.

From Table III, one sees that the number to be compared with that of the preceding paragraph is $\tau_{m.d.}=(1.4\times10^{-2})/0.64=2.2\times10^{-2}$ sec. The reasons for this apparent discrepancy of a factor of three are not known, but it can be pointed out that a factor of about this size turns up in both $CaF_2:Tm^{2+}$ and $CaF_2:Dy^{2+}$ when analogous comparisons are made.

[24] G. S. Ofelt (private communication).

THE PREPARATION AND OPTICAL SPECTRA OF $SrCl_2:Sm^{2+}$: EXPERIMENTAL PROCEDURES

Divalent samarium was incorporated into $SrCl_2$ by the addition of the desired amounts of $SmCl_3$ and Sm metal in the proper stoichiometric ratio. The material was melted in graphite crucibles in an inert atmosphere and single crystals grown by pulling from the melt or by the Stockbarger technique. The material, being somewhat hygroscopic, cannot be exposed to ambient atmospheric moisture for more than a few seconds without attack.

The absorption spectra were measured on a Cary Model 14 double beam recording spectrophotometer. The fluorescence spectra was excited by a high-pressure mercury lamp (PEK 109) suitably filtered to remove wavelengths longer than about 6000 Å. Most of the spectra were observed with a Jarrell-Ash 0.5M Ebert scanning spectrometer in first order with a 30 000 lines per inch grating and a Dumont 6911 photomultiplier tube. The relative spectral response of the combined optical and detection system was determined from a calibrated tungsten source. The linewidth measurements were performed on a 1M Ebert spectrometer with a 7500 lines per inch Harrison grating to obtain a resolution of ~0.05 Å. Lifetimes of the emitted light were measured by illuminating the crystal with a 20-μsec pulsed flash from an FX-11 xenon lamp and observing the decay of the photocurrent of a selected monochromatic band of fluorescent radiation on an oscilloscope display.

In an effort to insure that all of the observed fluorescence was due to divalent Sm, several crystals with total Sm concentrations up to 0.3% were investigated. In one the proportion of trivalent Sm was very greatly enhanced by treatment with oxygen at high temperatures. In none of the samples were there significant differences in the observed fluorescence spectra although some of the weakest features were not observed in the most concentrated samples.

ACKNOWLEDGMENTS

The authors wish to thank especially J. E. Scardefield and C. J. Lent for the preparation of $SrCl_2:Sm^{2+}$ crystals, and J. R. Lankard and G. D. Pettit for their assistance in the optical measurements. Discussions with Dr. S. P. Keller, Dr. P. Weller, and Dr. W. V. Smith were helpful.